| | |
|---|---|
| Title | Holographic arrays based on semiconductor microstructures |
| Author(s) | Liew, Timothy Chi Hin |
| Citation | Liew, T. C. H. (2012). Holographic arrays based on semiconductor microstructures. Physical Review B, 86(23), 235314-. |
| Date | 2012 |
| URL | http://hdl.handle.net/10220/43889 |
| Rights | © 2012 American Physical Society. This paper was published in Physical Review B and is made available as an electronic reprint (preprint) with permission of American Physical Society. The published version is available at: [http://dx.doi.org/10.1103/PhysRevB.86.235314]. One print or electronic copy may be made for personal use only. Systematic or multiple reproduction, distribution to multiple locations via electronic or other means, duplication of any material in this paper for a fee or for commercial purposes, or modification of the content of the paper is prohibited and is subject to penalties under law. |

# Holographic arrays based on semiconductor microstructures

T. C. H. Liew
*Mediterranean Institute of Fundamental Physics, 31, via Appia Nuova, Rome 00040, Italy*
(Received 17 October 2012; published 26 December 2012)

A concept of complex reflectivity modulation is proposed based on the electrical control of quantum well exciton resonances that influence the propagation of light in a layered semiconductor structure. By variation in exciton energies, both the intensity and the phase of reflected light can be fully controlled. Unlike previous devices, for full complex light modulation, the design is based on a single device in a single structure. The device allows complete 100% intensity contrast and allows for the construction of small pixel sizes with fast response times.

DOI: 10.1103/PhysRevB.86.235314 PACS number(s): 71.36.+c, 42.79.Hp, 71.35.−y, 85.60.Pg

## I. INTRODUCTION

Electronically controlled spatial light modulators, that vary the amplitude or phase of light, have given rise to a variety of optoelectronic technologies, such as high-speed optical switches and filters, as well as tunable lenses suitable for autofocus cameras, adaptive three-dimensional imaging,[1] and light steering.[2] In addition, increases in computational power are set to enable the emerging technology of computer-generated holography,[3] useful for displays, data transmission, data storage,[4] and optical tweezers.[5] Due to hardware restrictions, most existing routes rely on phase-only modulation, which requires intensive algorithms for holographic fringe pattern calculation.[6] Hardware capable of independent variation in phase and amplitude is expected to allow more flexibility in system designs and to improve performance characteristics.[7]

Earlier methods for the simultaneous modulation of amplitude and phase have been based on liquid-crystal spatial light modulators where one can consider the alignment of two spatial light modulators,[8,9] the use of double-pass configurations,[10,11] or the encoding of complex light over multiple pixels.[12–14] A recent technology is based on a combination of four liquid-crystal pixels arranged into a "superpixel" of size $(2 \times 19\ \mu\text{m})^2$.[15] Despite their versatility,[16] liquid crystals typically have limited response times. The response times of ferroelectric liquid crystals are inversely proportional to the applied voltage and achieve values of $\tau_r \sim 4$ ms for moderate electric fields $\sim$130 kV/cm (Ref. 17). For faster spatial light modulation, digital micromirror devices ($\tau_r \sim 20\ \mu$s) (Ref. 18) and blue-phase liquid crystals ($\tau_r \sim \mu$s) (Ref. 19) have been developed. Also, for beam switching applications, acousto-optic modulators can respond within the time taken for phonons to cross the beam, which may be in the 5–100-ns range. However, devices capable of independent amplitude and phase modulation based on these systems have not been considered, probably due to the likely necessity of coupling together multiple devices requiring very careful alignment.

Here, an alternative scheme of amplitude and phase modulation is considered based on the interaction between quantum well excitons and light propagating in a distributed Bragg reflector. Unlike previous devices, simultaneous analog control of the amplitude and phase of emission is arranged in a single compact solid-state microstructure. The device has no moving parts, unlike micromirror devices, and does not rely on pulse width modulation (temporal multiplexing). The pixels of the device can be arranged by laterally patterning the system into quantum boxes. From the available technologies: Bragg reflector layer thickness variation,[20] metal surface patterning,[21] or micropillar etching[22] are all capable of micron-sized pixels. The device is based on electrically controlled modulation of the reflectivity. The intrinsic time scale of the system is the exciton lifetime, which is fast in the range of a few picoseconds such that repetition rates will more likely be limited by external factors, such as time scales of the control electronics.

It is well known that the (complex) reflection coefficient of light, of frequency $\omega$, incident on an exciton resonance in a quantum well follows the Lorentzian-type line shape given by[23]

$$r_{\text{QW}} = \frac{i\Gamma_0}{\omega_0 - \omega - i(\gamma + \Gamma_0)}, \tag{1}$$

where $\Gamma_0$ is the radiative broadening, $\omega_0$ is the exciton frequency, and $\gamma$ is the homogeneous broadening.

Since the exciton frequency can be controlled by electric[24,25] or magnetic fields,[26] one has a pixel capable of the modulation of the amplitude and phase or reflected light. However, since there is only one variable $\omega_0$, it is not possible to control the intensity and phase independently with a single resonance. Furthermore, the phase does not vary over the complete range of 0 to $2\pi$. To circumvent these problems, a design based on the simultaneous excitation of two exciton resonances is considered. Through independent variation in the energies of each resonance, intensities and phases can be chosen arbitrarily with the phase extending over a full $2\pi$ range.

## II. SCHEME

A scheme for the construction of a device with two independently tunable exciton resonances is shown in Fig. 1. Alternating layers of refractive index [e.g., AlGaN/AlInN (Ref. 27)] form DBRs, and a central layer forms a cavity that confines light. The top layer of the structure is coated in metal (e.g., gold, aluminum, or silver[28,29]). Similar to the design of Ref. 30, quantum wells (QWs) are grown within the Bragg mirror layers, and Fig. 1 considers a case where two quantum wells are grown in different layers near the top of the structure. The use of GaN quantum wells allows one to work with exciton

 

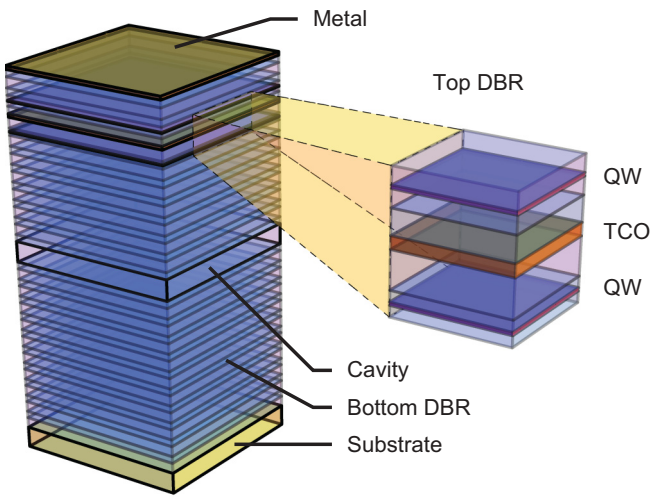


FIG. 1. (Color online) Scheme of a complex spatial light modulator based on distributed Bragg reflectors (DBRs), two QWs, and two conducting layers. Note that the illustration is not to scale and that, in reality, the lateral size of the pixel would exceed the total thickness of the semiconductor layers. It is assumed that the conducting layers can be independently connected to control electronics (not shown).[28,31,32]

resonances at room temperature. A second conducting layer is placed in the structure between the two quantum wells. The purpose of this layer is to apply electric fields with different voltages across the two different quantum wells. In principle, this layer could also be made from metal, in which case, the system is similar to the double-metal contact devices that are in development for polariton lasers.[28,31,32] However, it should be pointed out that only a few structures have been successfully grown with metal layers between other layers in the system, for example, in a pioneering paper where organic layers acted as spacers.[33] In GaN-based systems, the use of a transparent conductive oxide (TCO), such as indium tin oxide is perhaps a more-established technique.[34,35] This layer can be grown with a thickness matching the Bragg reflector periodicity, thus, forming an integral part of the structure while able to connect to an external voltage.

Given that the gold layers are neighbored by undoped semi-insulating material, the charge of the conducting layers can be varied independently through the engineering of metal contacts (not shown in the figure). The charged layers, with lateral size exceeding the size of the cavity in the growth direction, each contribute a roughly uniform electric field given by $F_{1,2} = \sigma/(2\epsilon)$, where $\sigma$ is the uniform charge density and $\epsilon$ is the permittivity. If the conducting layers have the same sign of charge, then the electric field experienced by the upper quantum well is given by the difference $F_2 - F_1$, whereas, that of the lower quantum well is given by the sum $F_1 + F_2$. Thus, the electric field of each quantum well can be independently varied by varying the charge of the conducting layers. Applied electric fields allow control of the resonance energy of excitons within each quantum well via the quantum-confined Stark effect over a range of ~75 meV.[36]

The distribution of the optical field in the whole structure can be found from the transfer-matrix technique[23] and is shown in Fig. 2(a) for the case where the quantum well exciton resonances are strongly detuned (blue solid curve)

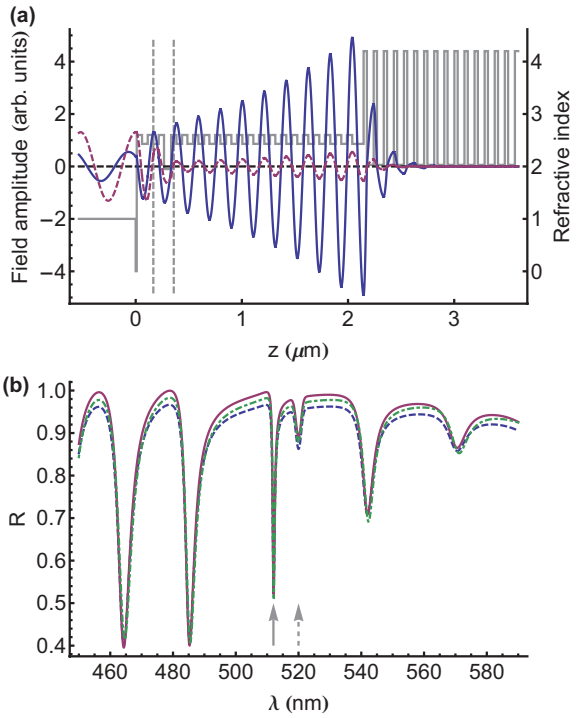


FIG. 2. (Color online) (a) Distribution of the real part of the optical-field amplitude in the structure considered in Fig. 1 with quantum well excitons detuned (blue solid curve) and resonant (purple dashed curve) with the cavity mode energy. The variation in the refractive index of the system is shown in gray, and the vertical dashed lines mark the positions of the quantum wells. The angle of incidence was chosen as 10°. (b) Reflectivity of the system for TE (purple solid) and TM (blue dashed) polarizations. The green dot-dashed curve shows what the TE reflectivity would be with the top metal layer removed. The gray arrows mark the cavity mode wavelength (solid) and quantum well exciton wavelength (dashed).

and resonant with the cavity mode (purple dashed curve). Realistic parameters were chosen corresponding to a GaN-based system with the Bragg mirror after the cavity made from $Si/SiO_2$ layers,[27] which have a higher refractive index contrast. To allow for straightforward separation of the incident and reflected fields, the system is excited at an angle of incidence of 10°. Note that, although the majority of light is trapped near the cavity layer, there is still a significant intensity at the position of the quantum wells. As is seen in Fig. 2(a), the tuning of the exciton resonances can then have a significant effect on the amplitude and phase of the reflected light.

To account for the inhomogeneous broadening of excitons $\Delta$ caused by disorder, Eq. (1) was modified[37]

$$r_{\mathrm{QW}} = -\frac{\sqrt{\pi}\Gamma_0 w(z)}{\Delta + \sqrt{\pi}\Gamma_0 w(z)}, \tag{2}$$

where $w(z) = e^{-z^2}\mathrm{erfc}(-iz)$ and $z = (\omega - \omega_0 + i\gamma)/\Delta$. The values for the inhomogeneous (5 meV), homogeneous (0.1 meV), and radiative broadening (0.4 meV) in GaN quantum wells were taken from Ref. 37.

Figure 2(b) shows the dependence of the reflectivity of the system on the frequency of light. The quantum well resonances are tuned within the stop band of the DBR mirror, and the light

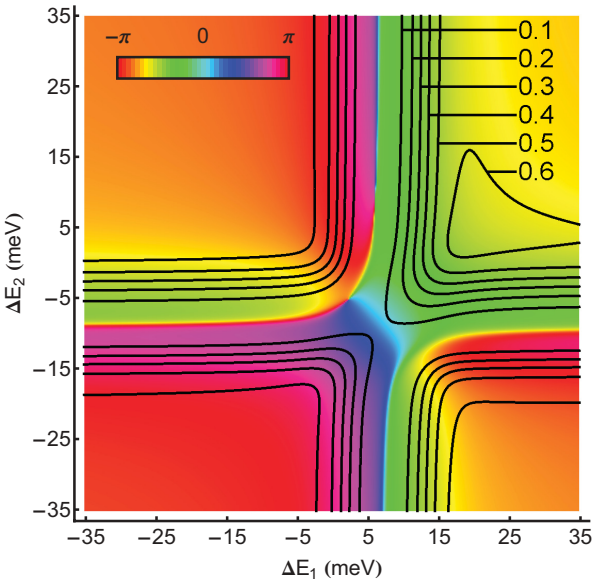


FIG. 3. (Color online) Variation in the reflected intensity (contours) and phase (color scale) of the system with $E_1$ and $E_2$. In the absence of an electric field, the quantum well energies are chosen at the center of the stop band of the DBR reflector $\hbar\bar{\omega}$, marked by the dashed gray arrow in Fig. 2(b). $\Delta E_1$ and $\Delta E_2$ represent the electric-field-induced shift in the exciton energies from this value. The light frequency was chosen at the cavity resonance frequency [gray arrow in Fig. 2(b)].

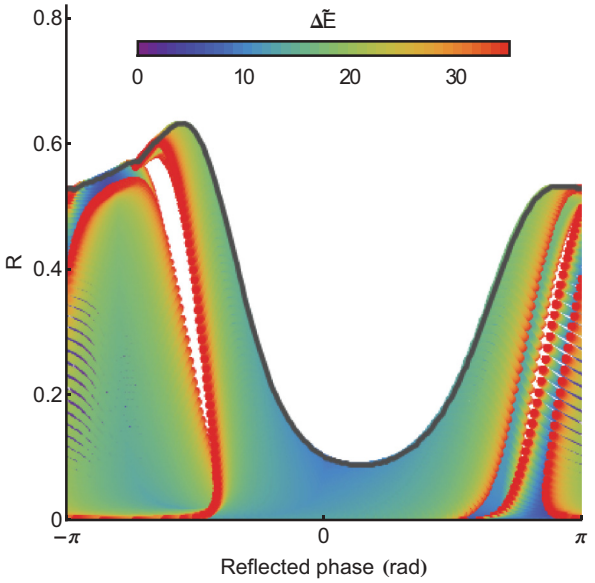


FIG. 4. (Color online) Reflected intensity coefficients ($R$) and phases for variation in $E_1$ and $E_2$ over a range of 35 meV. The spacing of the spots indicates the accessible points with variations in $E_1$ and $E_2$ in steps of 0.2 meV. The color scale shows the value of $\widetilde{\Delta E}$, defined in the text, for each point.

frequency is chosen to be resonant with the cavity mode at the frequency marked by the gray arrow. Due to the nonzero angle of incidence, the reflectivity is slightly different in the TE and TM polarizations. For simplicity, we will consider the TE polarization throughout the rest of this paper. The presence of the top metal layer has a small effect on the reflectivity [the green dot-dashed curve in Fig. 2(a) shows the case of no top metal layer]. By choosing a thin layer (10 nm), the losses due to absorption in the metal are minimal. They were accounted for by using the Drude model, which gives rise to a complex refractive index.[38] Absorption losses due to the TCO layer were also accounted for.

## III. ELECTRICAL DEPENDENCE OF COMPLEX REFLECTION COEFFICIENT

The modification of the complex reflection coefficient by varying quantum well energies $E_1$ and $E_2$ can also be found from the transfer-matrix technique. Figure 3 shows the typical variation in the phase (colors) and intensity (contours). Due to the appearance of a vortex-type structure in the $E_1$-$E_2$ plane, it is notable that the variation in $E_1$ and $E_2$ over a range not exceeding 0.35 meV gives access to a variety of reflected phases and intensities.

Given the freedom of phases and intensities indicated by Fig. 3, the possibility of full complex modulation of the reflected field is assessed by plotting the available combinations of intensity and phase. This is shown in Fig. 4, using steps of 0.2 meV for $E_1$ and $E_2$. The color scale shows the quantity $\widetilde{\Delta E} = \max\{|E_1 - \hbar\bar{\omega}|, |E_1 - \hbar\bar{\omega}|\}$, which is an indication of the energy shift applied to the excitons in the two quantum wells—red represents a large shift, whereas, blue represents a small shift. It can be seen that a continuum of possibilities exists below $R = 0.1$. In this region, by recording the intensity and phase for different values of $E_1$ and $E_2$, a lookup table of values could be constructed, linking each desired value of intensity and phase to a pair of input voltages. The full range of phase ($2\pi$) is accessible and, since points can be chosen with near-zero-reflected intensity, 100% contrast is achievable. The white regions above the gray curve in Fig. 4 show inaccessible intensities and phases with the present scheme. The white regions below these curves are not accessible using an exciton shift of up to 35 meV, however, they can be covered by larger exciton shifts.

The change in the reflectivity, depending on the exciton resonance tuning, is a consequence of the absorption of light by excitons in the quantum wells. Although part of this light would be reemitted by stimulated emission processes from the excitons and would appear in the reflected signal, a remaining part of the light would contribute a photoluminescence. This can be separated from the reflected signal by spatial filtering (the reflected signal is emitted at a certain angle) and, if necessary, additional energy and polarization filtering.

The neglect of spatial dispersion effects assumes that only one confined mode is excited in each pixel, which requires a monochromatic optical field with the correct spatial profile. For a large pixel, a uniform incident field would be required to excite a single mode in reciprocal space. To demonstrate the principle of operation, it was assumed that the applied electric field modifies only the exciton energy. In reality, the values of $\Gamma_0$, $\gamma$, and $\Delta$ could also depend on the applied electric field. A more detailed treatment with self-consistent calculations, including the dependence of all parameters on the field-dependent exciton wave functions, would be more accurate and can be expected to slightly modify Fig. 4. However,

provided the qualitative feature of Fig. 4—it encompasses a full range of phases and intensities—remains, the scheme of the proposed device does not change. The presented results also neglect nonlinear effects, such as exciton-exciton interactions and are, thus, valid in the linear regime of moderate light intensity. Recalibration with an additional nonlinear shift in the exciton resonance would be needed for a high-intensity operation. Finally, it was also assumed that each pixel can act independently and that exciton tunneling between pixels was negligible. When considering the whole array structure, corrections due to the electric fields applied to neighboring pixels might need consideration for small pixel spacings. In principle, these corrections could be calculated by a control algorithm.

## IV. CONCLUSION

A device for complex spatial light modulation, with independent control of intensity and phase, is proposed. The presence of quantum wells inside a distributed Bragg reflector can significantly influence the reflectivity due to the interaction of light with exciton resonances. The use of metal/transparent-conducting oxide layers, grown as part of the structure, allow the application of electric fields that shift the exciton resonance energies within the quantum wells via the quantum-confined Stark effect. Through the variation in exciton energies in two different quantum wells, a full range of phases ($2\pi$) can be imposed on the reflected optical field, together with an independent choice of intensities over a range supporting 100% contrast.

It should be stressed that the complex (intensity and phase) spatial light modulation is achieved in a single semiconductor heterostructure, which is not possible with other technologies. Indeed, the possibility of pixels of typical size 5–10 $\mu$m is similar to (or slightly better than) what is achievable with digital micromirror or liquid-crystal technologies. However, for these technologies to give complex spatial light modulation, one must couple multiple devices, resulting in a macroscopic size that is challenging to align. In addition, the proposal of this paper avoids the need to wait for moving parts as in digital micromirror devices or the reorientation of liquid crystals such that fast response times are expected. A typical exciton lifetime, around a few picoseconds,[37] would allow repetition rates in the 10–100-GHz range.

## ACKNOWLEDGMENTS

Encouraging discussions with T. Espinosa-Ortega and P. S. Eldridge were greatly appreciated. This work was supported by the EU Marie-Curie project EPOQUES.

[1] N. A. Riza, M. Sheikh, G. Webb-Wood, and P. G. Kik, Opt. Eng. **47**, 063201 (2008).
[2] J.-J. Chen and K.-H. Cheng, Opt. Eng. **49**, 053003 (2010).
[3] C. Slinger, C. Cameron, and M. Stanley, Computer **38**, 46 (2005).
[4] D. Psaltis and G. Burr, Computer **31**, 52 (1993).
[5] A. Ashkin, J. M. Dziedzic, J. E. Bjorkholm, and S. Chu, Opt. Lett. **11**, 288 (1986).
[6] A. Georgiou, T. D. Wilkinson, N. Collings, and W. A. Crossland, J. Opt. A, Pure Appl. Opt. **10**, 015306 (2008).
[7] L. G. Neto, P. S. Cardona, G. A. Cirino, R. D. Mansano, and P. B. Verdonck, J. Microlithogr., Microfabr., Microsyst. **2**, 96 (2003).
[8] L. G. Neto, D. Roberge, and Y. Sheng, Appl. Opt. **35**, 4567 (1996).
[9] T. Kelly and J. Munch, Appl. Opt. **37**, 5184 (1998).
[10] R. Dou and M. K. Giles, Appl. Opt. **35**, 3647 (1996).
[11] S. Chavali, P. M. Birch, R. Young, and C. Chatwin, Opt. Laser. Eng. **45**, 413 (2007).
[12] V. Bagnoud and J. D. Zuegel, Opt. Lett. **29**, 295 (2004).
[13] V. Arrizón, Opt. Lett. **28**, 1359 (2003).
[14] P. Birch, R. Young, D. Budgett, and C. Chatwin, Opt. Lett. **25**, 1013 (2000).
[15] E. G. van Putten, I. M. Vellekoop, and A. P. Mosk, Appl. Opt. **47**, 2076 (2008).
[16] J. Beeckman, K. Neyts, and P. J. M. Vanbrabant, Opt. Eng. **50**, 081202 (2011).
[17] N. A. Clark and S. T. Lagerwall, Appl. Phys. Lett. **36**, 899 (1980).
[18] G. A. Feather and D. W. Monk, *Proceedings, Seventh Annual IEEE International Conference of Wafer Scale Integration* (IEEE, Piscataway, NJ, 1995), p. 43.
[19] Y. Hisakado, H. Kikuchi, T. Nagamura, and T. Kajiyama, Adv. Mater. **17**, 96 (2005).
[20] O. El Daïf, A. Baas, T. Guillet, J.-P. Brantut, R. Idrissi Kaitouni, J. L. Staehli, F. Morier-Genoud, and B. Deveaud, Appl. Phys. Lett. **88**, 061105 (2006).
[21] C. W. Lai, N. Y. Kim, S. Utsunomiya, G. Roumpos, H. Deng, M. D. Fraser, T. Brynes, P. Recher, N. Kumada, T. Fujisawa, and Y. Yamamoto, Nature (London) **450**, 529 (2007).
[22] D. Bajoni, E. Peter, P. Senellart, J. L. Smirr, I. Sagnes, A. Lemaître, and J. Bloch, Appl. Phys. Lett. **90**, 051107 (2007).
[23] A. V. Kavokin and G. Malpuech, *Cavity Polaritons* (Elsevier, New York, 2003).
[24] I. A. Shelykh, R. Johne, D. D. Solnyshkov, and G. Malpuech, Phys. Rev. B **82**, 153303 (2010).
[25] T. C. H. Liew, A. V. Kavokin, T. Ostatnický, M. Kaliteevski, I. A. Shelykh, and R. A. Abram, Phys. Rev. B **82**, 033302 (2010).
[26] Y. Zhang and G. Jin, Phys. Rev. B **79**, 195304 (2009).
[27] G. Christmann, R. Butté, E. Feltin, J-F. Carlin, and N. Grandjean, Phys. Rev. B **73**, 153305 (2006).
[28] R. Butte and N. Grandjean, Semicond. Sci. Technol. **26**, 014030 (2011).
[29] K. Okamoto, I. Niki, A. Shvartser, Y. Narukawa, T. Mukai, and A. Scherer, Nat. Mater. **3**, 601 (2004).
[30] J. Bloch, T. Freixanet, J. Y. Marzin, V. Thierry-Mieg, and R. Planel, Appl. Phys. Lett. **73**, 1694 (1998).
[31] D. Solnyshkov, E. Petrolati, A. Di Carlo, and G. Malpuech, Appl. Phys. Lett. **94**, 011110 (2009).
[32] I. Iorsh, M. Glauser, G. Rossbach, J. Levrat, M. Cobet, R. Butté, N. Grandjean, M. A. Kaliteevski, R. A. Abram, and A. V. Kavokin, Phys. Rev. B **86**, 125308 (2012).

[33]R. Brückner, M. Sudzius, S. I. Hintschich, H. Fröb, V. G. Lyssenko, M. A. Kaliteevski, I. Iorsh, R. A. Abram, A. V. Kavokin, and K. Leo, Appl. Phys. Lett. **100**, 062101 (2012).
[34]T.-C. Lu, C.-C. Kao, H.-C. Kuo, G.-S. Huang, and S.-C. Wang, Appl. Phys. Lett. **92**, 141102 (2008).
[35]Y. Higuchi, K. Omae, H. Matsumura, and T. Mukai, Appl. Phys. Express **1**, 121102 (2008).
[36]T. Takeuchi, C. Wetzel, S. Yamaguchi, H. Sakai, H. Amano, I. Akasaki, Y. Kaneko, S. Nakagawa, Y. Yamaoka, and N. Yamada, Appl. Phys. Lett. **73**, 1691 (1998).
[37]G. Malpuech and A. Kavokin, Appl. Phys. Lett. **76**, 3049 (2000).
[38]M. E. Sasin, R. P. Seisyan, M. A. Kaliteevski, S. Brand, R. A. Abram, J. M. Chamberlain, A. Yu. Egorov, A. P. Vasil'ev, V. S. Mikhrin, and A. V. Kavokin, Appl. Phys. Lett. **92**, 251112 (2008).